

IL NUOVO CIMENTO **38 C** (2015) 199  
DOI 10.1393/ncc/i2015-15199-5

COLLOQUIA: LaThuile15

## Top quark studies at the Tevatron

S. LEONE for the CDF and D0 COLLABORATIONS

*INFN, Sezione di Pisa - Pisa, Italy*

received 2 October 2015

**Summary.** — A selection of the most recent CDF and D0 results in the top quark sector is presented. The top quark pair production and single top production and cross section measurements are discussed. The  $t\bar{t}$  charge asymmetry results are shown. The most recent top quark mass measurements and the Tevatron combined top quark mass are illustrated.

PACS 14.65.Ha – Top quarks.

### 1. – Introduction

The Tevatron Collider provided  $p\bar{p}$  collisions at a center of mass energy of  $\sqrt{s} = 1.96$  TeV until it ceased operating in September 2011. Data corresponding to approximately  $10 \text{ fb}^{-1}$  of integrated luminosity were recorded by the CDF and D0 experiments. The top quark was first observed at the Tevatron. On March 2nd, 1995, physicists at CDF and D0 announced the discovery of the top quark [1]. Since then, the experimental top quark physics started.

At the Tevatron center of mass energy top quarks are primarily produced in  $t\bar{t}$  pairs via strong processes, with the  $q\bar{q} \rightarrow t\bar{t}$  annihilation being the dominant one, exactly the opposite than the production at the LHC, where the dominant process is the gluon fusion  $gg \rightarrow t\bar{t}$ . Therefore Tevatron is the right place to study the  $q\bar{q}$  annihilation in  $t\bar{t}$  production.

The standard model of elementary particles (SM) predicts that top quarks can be produced also singly, through electroweak  $s$ -channel or  $t$ -channel exchange of a virtual  $W$  boson, with a predicted cross section about half that of top quark pair production. Single top associated production  $Wt$  is also possible, but at the Tevatron the expected cross section for this process is very small and it is not measurable by itself.

Single top quark production was observed for the first time at the Tevatron in 2009 [2]. It took 14 years after the top quark discovery for the single top to be observed.

In the SM each top quark decays almost exclusively into a real  $W$  and a  $b$  quark. Each  $W$  subsequently decays into either a charged lepton and a neutrino or two quarks.

For top quark pair production, events can thus be identified by means of different combinations of leptons ( $e$  or  $\mu$ ) and jets. Mainly two decay modes are used in the analyses described in this report: the dilepton mode, where both  $W$ 's decay to a charged lepton and a neutrino, and the lepton plus jets mode, where one  $W$  decays leptonically and the other one decays hadronically to a pair of quarks.  $b$ -jets are always present in the final state.

The top quark is the most massive of the known elementary particles. As a consequence of its large mass it is the only quark that decays before hadronizing, thus offering a chance to study a bare quark. The top quark properties can be inferred from the kinematic distributions of its decay products. With a Yukawa coupling near one, the top quark could play a special role in electroweak symmetry breaking, and its large mass could potentially lead to enhanced couplings to new physics.

Since the top quark discovery, Tevatron experiments tried to answer the question if the observed top quark was the standard model one, because deviations of the measured top quark properties from the SM prediction would be a signal of new physics. All the analyses described in the following are based on the full Tevatron Run II dataset.

## 2. – Top quark pair production cross section

The  $t\bar{t}$  production cross section has been measured at the Tevatron in all the decay channels. We found consistent results among the different channels, the different methods used in the analyses and the two experiments. Measurements from CDF and D0 have been used to obtain a Tevatron combined cross section of  $\sigma_{t\bar{t}} = 7.60 \pm 0.41$  (stat + syst) pb [3] for a top quark mass  $M_{top} = 172.5 \text{ GeV}/c^2$ . The experimental uncertainty is 5.4% and it is dominated by the systematic uncertainty from the luminosity measurement and the signal modeling. The result is in good agreement with the SM expectation of  $\sigma_{t\bar{t}} = 7.35^{+0.28}_{-0.33}$  pb at NNLO+NNLL in perturbative QCD [4].

D0 recently published a measurement of the differential production cross section in the lepton plus jets channel, as a function of the invariant mass of the  $t\bar{t}$  pair  $M_{t\bar{t}}$ , the transverse momentum of the top quark  $P_T^{top}$  and the absolute value of the rapidity of the top quark  $y_{top}$  [5]. Figure 1 (left) shows the measured differential cross section as a function of  $P_T^{top}$ , for data compared to several QCD predictions. Figure 1 (right) shows the ratio of data, ALPGEN [6] (dashed line) and MC@NLO [7] cross sections (dash-dotted line) to the QCD prediction at approximate NNLO [8]. The differential cross sections are measured with a typical precision of 9%, and are in general good agreement with predictions obtained by QCD generators and predictions at approximate NNLO.

## 3. – $t\bar{t}$ charge asymmetry

The  $t\bar{t}$  production mechanism has been investigated in details by studying the charge production asymmetry. The asymmetry is such that the top quark is preferentially emitted in the direction of the incoming light quark, while the antitop quark follows the direction of the incoming antiquark. A recent QCD NNLO calculation evaluates an asymmetry of 9.5% [9]. The  $gg$  initial state does not contribute to the asymmetry but dilutes the average value. On the other hand, new physics could give rise to an enhanced asymmetry.

Experimentally the asymmetry is based either on the fully reconstructed top quarks or on leptons from the  $W$  decay. In the first case it uses the rapidity difference  $\Delta y$  of the top (antitop) quark decaying semileptonically  $t \rightarrow l\nu b$  and the antitop (top) decaying

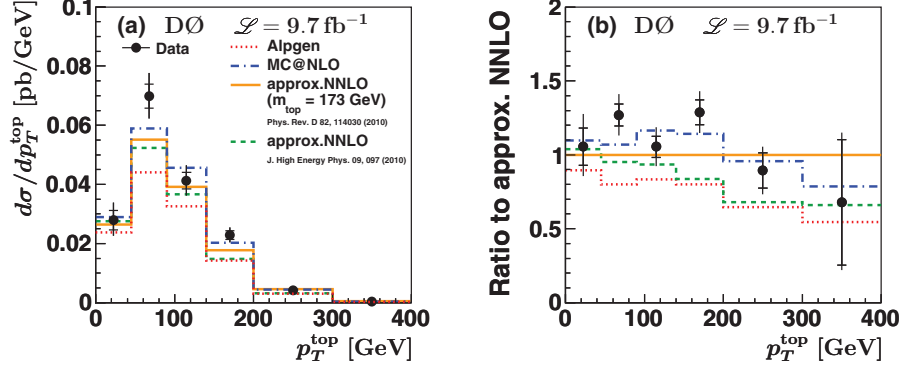


Fig. 1. – (left): D0 measured  $t\bar{t}$  differential cross section as a function of  $P_T^{top}$ ; (right): ratio of data, ALPGEN (dashed line) and MC@NLO cross sections (dash-dotted line) to the QCD prediction at approximate NNLO.

hadronically  $\bar{t} \rightarrow jjb$  (this observable is independent of effects affecting the top decay). In the second case the lepton asymmetry in  $t\bar{t}$  decay is parametrized as a function of  $qy_\ell$  where  $q$  is the charge and  $y_\ell$  is the rapidity of the charged lepton from the  $W$  decay: there is no need to reconstruct the  $t\bar{t}$  system therefore this quantity is insensitive to biases from the top reconstruction procedure.

**3.1. Top-antitop rapidity asymmetry.** – The top-antitop rapidity asymmetry has been measured by CDF and D0 both in the lepton plus jets and dilepton channels. After measuring the rapidity difference  $\Delta y$ , we subtract the non- $t\bar{t}$  background and correct for acceptance and detector resolution effects, in order to obtain the parton level (or production level) rapidity difference distribution. Figure 2 (left) shows the CDF differential cross section after correction to the parton level compared to the SM prediction. CDF measures an asymmetry  $A_{\ell+jets}^{FB} = (16.4 \pm 4.5)\%$  [10].

D0 recently updated this measurement on the full Run II dataset, using a new kinematic fitting algorithm for events with 4 or more jets and a new partial reconstruction

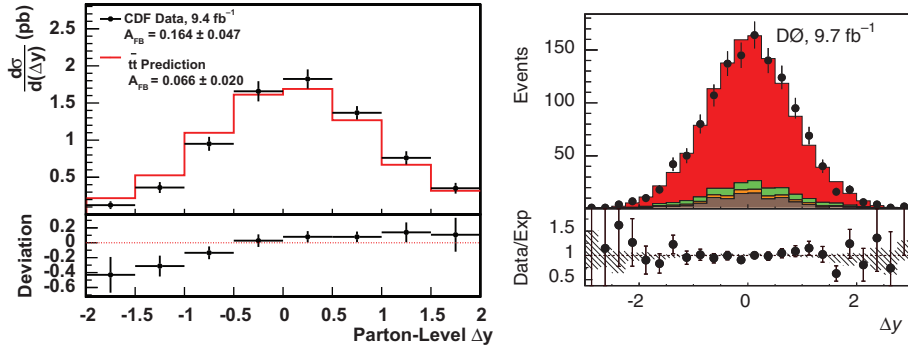


Fig. 2. – (left): CDF  $d\sigma/d(\Delta y)$  as measured in the data after correction to the parton level, compared to the SM prediction; (right): D0  $\Delta y$  distribution of  $t\bar{t}$  candidates at reconstruction level.

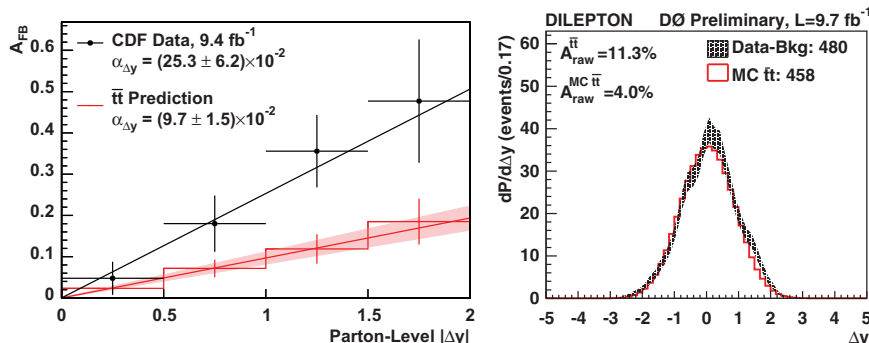


Fig. 3. – (left): CDF parton-level forward-backward asymmetry as a function of  $|\Delta y|$ . A best-fit line is superimposed. The shaded region represents the theoretical uncertainty on the slope of the prediction; (right): D0  $\Delta y$  distribution of the  $t\bar{t}$  dilepton candidates obtained after subtracting the background contribution.

algorithm for events with only 3 jets. Events are separated in several sub-channels, based on the number of jets and the number of  $b$ -tags [11]. Figure 2 (right) shows the reconstructed  $\Delta y$  distribution for events with at least 4 jets and 2  $b$ -tags. D0 measures an asymmetry  $A_{\ell+jets}^{FB} = (10.6 \pm 3.0)\%$ , consistent with NLO and NNLO predictions [9, 12].

Both experiments studied the kinematic dependence of the asymmetry from the  $M_{t\bar{t}}$  and  $\Delta y$  distributions. Figure 3 (left) shows the CDF parton-level forward-backward asymmetry as a function of  $|\Delta y|$ . The observed kinematic dependencies in CDF data are slightly larger than what predicted by the SM at both NLO and NNLO.

D0 recently presented a measurement of the asymmetry obtained in the dilepton channel, using a matrix element technique that calculates the likelihood of the possible  $t\bar{t}$  kinematic configurations per event [13]. Figure 3 (right) shows this probability distribution as a function of  $\Delta y$ . After background subtraction and calibration back to partonic level D0 measures an asymmetry  $A_{\ell\ell}^{FB} = (15.0 \pm 6.4 \text{ (stat)} \pm 4.9 \text{ (syst)})\%$ .

**3.2. Lepton asymmetry.** – There is a significant correlation between the direction of the top quark and its decay products, so that an asymmetry in the parent top quark direction will induce an asymmetry in the particles resulting from its decay. Experimentally the direction of a lepton is determined with greater precision than that of a top quark, thus corrections for detector acceptance and experimental resolution are simpler to estimate. Figure 4 (left) shows the CDF binned lepton asymmetry as a function of  $|qy_\ell|$ , measured in the lepton plus jets channel after correcting for acceptance and detector effects, compared to NLO QCD predictions. CDF measures an asymmetry  $A_{\ell+jets}^\ell(qy_\ell) = (9.4 \pm 2.4 \text{ (stat)} \pm_{-1.7}^{+2.2} \text{ (syst)})\%$  [14].

D0 categorizes the events selected in the lepton plus jets channel in several sub-samples identified by the number of jets and  $b$ -tags [15]. The leptonic asymmetries are unfolded to parton level separately in each channel and the measured asymmetry values are then combined to form the inclusive measurement. D0 measures an asymmetry  $A_{\ell+jets}^\ell = (4.2 \pm 2.3 \text{ (stat)} \pm_{-2.0}^{+1.7} \text{ (syst)})\%$ . Figure 4 (right) shows the D0 parton level lepton asymmetry by analysis channel. The solid vertical line is the MC@NLO prediction, and the vertical band indicates the combined value of 4.2% (dotted line) with its uncertainty of approximately 3%.

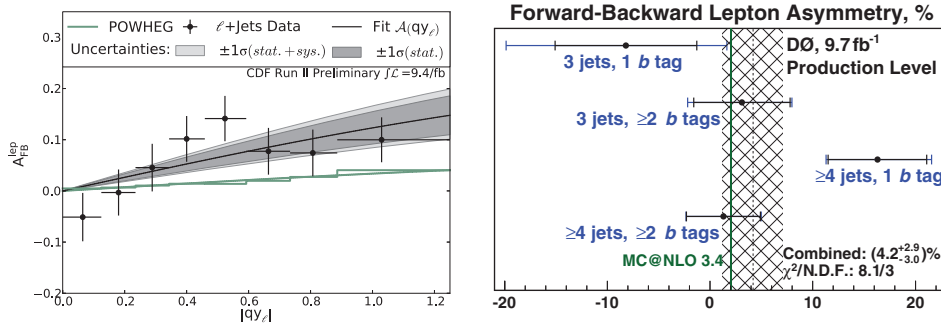


Fig. 4. – (left): CDF lepton asymmetry in the lepton plus jets channel after correcting for acceptance, compared to the NLO QCD prediction of POWHEG. The dark (light) gray bands indicate the statistical (total) uncertainty on the fit curve to the data; (right): D0 measured production-level  $A_{\ell+jets}^{\ell}$  by analysis channel. The vertical line shows the MC@NLO prediction.

#### 4. – Single top quark production

Single top quark production provides direct access to the  $Wtb$  vertex. The single top production cross section is proportional to the Cabibbo Kobayashi Maskawa (CKM) matrix element squared  $|V_{tb}|^2$ , therefore the measurement of the cross section allows a direct measurement of  $|V_{tb}|$ . In addition each channel of the single top quark production is sensitive to different classes of SM extensions: the  $t$ -channel process is more sensitive to flavor-changing neutral currents, while the  $s$ -channel is sensitive to contributions from additional heavy bosons [16]. Therefore, independently studying the production rate of these channels provides more restrictive constraints on SM extensions than just studying the combined production rate.

**4.1.  $s$ -channel production.** – Observing the  $s$ -channel process is more difficult, since the expected cross section is smaller than that of the  $t$ -channel and its kinematic features are less distinct from the background. However, the Tevatron has an advantage over the LHC in this mode, since valence quarks generally initiate  $s$ -channel single top quark production, leading to a larger signal-to-background ratio at the Tevatron than at the LHC. The CDF and D0 collaborations have reported evidence for  $s$ -channel production independently of each other [17]. The observation of the  $s$ -channel was obtained through the combination of the CDF and D0 measurements of the cross section [18]. The multivariate discriminants from CDF and D0, optimized to separate the  $s$ -channel signal from backgrounds, are combined by taking the product of their likelihoods and simultaneously varying the correlated uncertainties. The combined Tevatron discriminant for the  $s$ -channel is shown in fig. 5 (left). The expected  $s$ -channel signal contribution is shown by a filled blue histogram. The inset magnifies the region where most of the single top quark contribution is expected. The posterior probability distribution for the combination of the CDF and D0 analysis channels compared with the NLO+NNLL theoretical prediction [19] is shown in fig. 5 (right). The Tevatron measured  $s$ -channel cross section is  $\sigma_s = 1.29^{+0.26}_{-0.24}(\text{stat} + \text{syst})$  pb, with a significance corresponding to 6.3 standard deviations.

**4.2.  $s+t$  production.** – Recently CDF and D0 combined their measurements of the single top quark cross section for the production in the  $s+t$  channels [20]. The combination is obtained by collecting the multivariate discriminants inputs from both experiments for  $s$ -channel and  $t$ -channel and re-performing the statistical analysis (leading to a higher

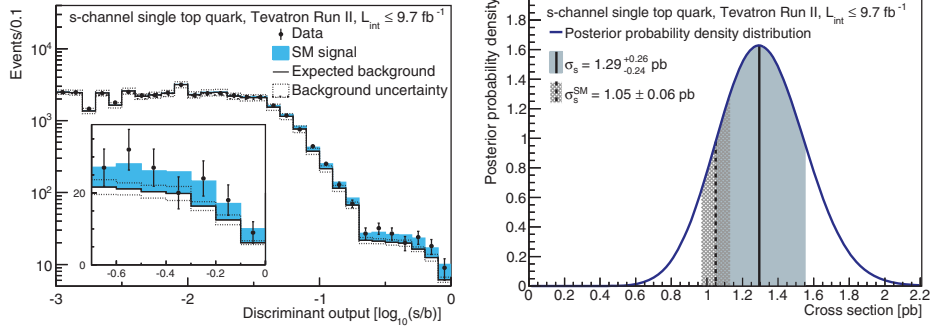


Fig. 5. – (left): Distribution of the CDF and D0  $s$ -channel discriminant histograms, summed for bins with similar signal-to-background ratio. The expected sum of the backgrounds is shown by the unfilled histogram, and the uncertainty of the background is represented by the gray shaded band. The expected  $s$ -channel signal contribution is shown by a filled blue histogram; (right): the posterior probability distribution for the combination of the CDF and D0 single top  $s$ -channel analyses compared with the theoretical prediction.

precision than just adding the single results). A two-dimensional posterior probability density is constructed as a function of  $\sigma_s$  and  $\sigma_t$  and is shown in fig. 6 (left). The measurement is shown with the one, two and three standard deviations probability contour and the SM expectation. Several BSM predictions are shown as well. The most probable value for the  $t$ -channel cross section is  $\sigma_t = 2.25^{+0.29}_{-0.31}$  (stat + syst) pb. The  $s + t$  cross section is measured by forming a two-dimensional posterior for  $\sigma_{s+t}$  vs.  $\sigma_t$  and then integrating over all possible values of  $\sigma_t$  with no assumption on the ratio of  $s$  and  $t$  channel. The Tevatron combined cross section is:  $\sigma_{s+t} = 3.30^{+0.52}_{-0.40}$  (stat + syst) pb.

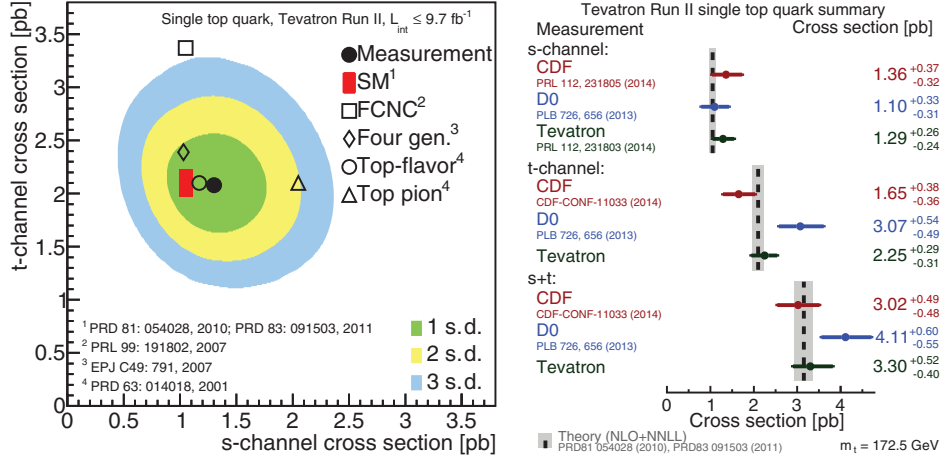


Fig. 6. – (left): Two-dimensional posterior probability density as a function of  $\sigma_t$  and  $\sigma_s$  with one, two, and three standard deviations probability contours for the combination of the CDF and D0 analysis channels, compared with the theoretical prediction of the SM; (right): Measured single top quark production cross sections from the CDF and D0 collaborations in different production channels and the Tevatron combinations of these analyses, compared with the theoretical prediction.

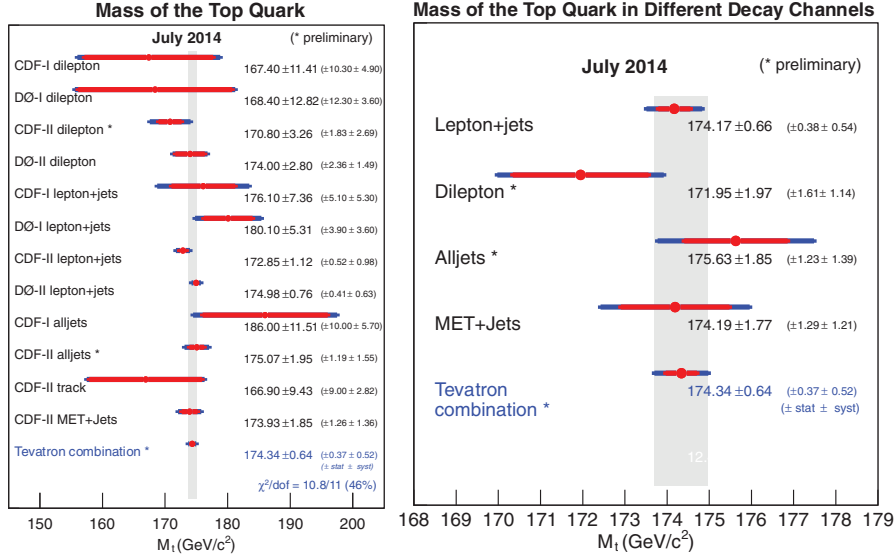


Fig. 7. – (left): Summary of the input measurements and resulting Tevatron average mass of the top quark. The red lines correspond to the statistical uncertainty while the blue lines show the total uncertainty; (right): summary of the combination of the twelve top-quark measurements by CDF and D0 for different final states.

The Tevatron CKM matrix element  $V_{tb}$  is extracted from a posterior probability density for  $|V_{tb}|^2$ , assuming a uniform prior probability distribution in the region of positive values. We obtain a lower limit on  $V_{tb} > 0.92$  at 95% C.L.

Figure 6 (right) shows a summary of the Tevatron single top quark cross section measurements. The grey vertical lines represent the NLO+NNLL theory predictions [19, 21]. The single top quark  $s + t$  cross section is measured at the Tevatron with a precision of 13%, while the  $s$ -channel production is measured with a precision of 19%.

## 5. – Top quark mass

The most measured top quark property is its mass, which is a free parameter of the SM. Several methods have been used to obtain precise top quark mass measurements, in all the decay channels. The most sensitive analyses from both CDF and D0 are performed in the lepton plus jets channel. Five Run I and seven Run II CDF and D0 top mass measurements have been combined to obtain the Tevatron top quark mass, which is limited by systematic uncertainties: the dominant ones are the signal modeling and the jet energy scale (JES) uncertainties [22]. Figure 7 (left) shows all the measurements used in the combination, while fig. 7 (right) shows the measured top quark mass in the different decay channels. The combined top mass is  $M_{top} = 174.34 \pm 0.37(\text{stat}) \pm 0.52(\text{syst}) \text{ GeV}/c^2$ . With a total uncertainty of  $0.64 \text{ GeV}/c^2$ , this measurement is already better than the world top quark mass presented in march 2014 which had an uncertainty of  $0.76 \text{ GeV}/c^2$  [23].

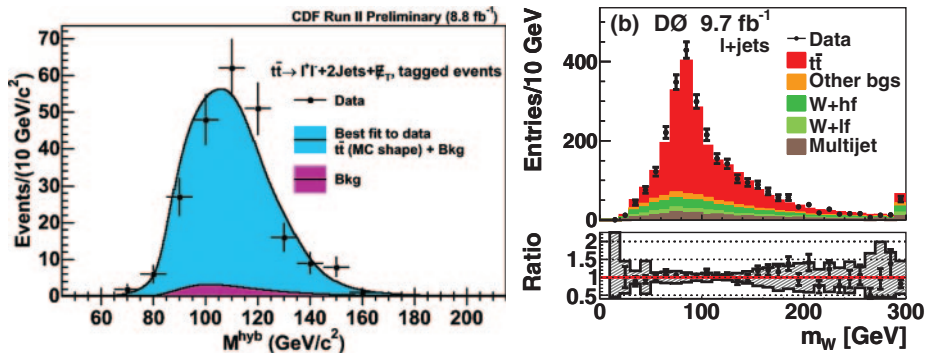


Fig. 8. – (left): CDF distribution of the variable  $M_{hyb}$  for dilepton  $b$ -tagged data and background and signal plus background probability distribution functions, normalized accordingly to the fit result; (right): D0 invariant mass of the jet pair matched to one of the  $W$  bosons in lepton plus jet events.

**5.1. Top quark mass in the dilepton channel.** – CDF recently updated the top quark mass measurement in the dilepton channel, using the full Run II dataset [24]. In the dilepton channel the statistics is not anymore the precision limiting factor, due to the large available dataset. The systematic uncertainty is dominated by the JES. This analysis was therefore conceived to minimize the influence of the jet-energy scale. It estimates the top quark mass by performing a fit of an observable to a sum of signal and background contributions. The choice of the observable has an impact on the precision of the measurement. In this analysis we use a hybrid variable defined as:  $M_{hyb} = wM_t^{reco} + (1 - w)M_{lb}^{alt}$ .  $M_t^{reco}$  is the reconstructed top quark mass (based on the neutrino  $\phi$ -weighting method [25]). The second variable, denoted as “alternative” mass  $M_{lb}^{alt}$ , is based only on lepton 4-momenta and jet directions, and  $w$  is a weighting parameter. By varying  $w$  from 0 to 1  $M_{hyb}$  varies from  $M_t^{reco}$  to  $M_{lb}^{alt}$ . The statistical and systematic uncertainties of the measurement depend on the choice of the  $w$  parameter. In order to find the optimal value of  $w$  we scan the  $[0,1]$  interval in steps of 0.05. For every point of the scan, we define the mass fit using the signal and background templates for  $M_{hyb}$  and evaluate the uncertainties. The optimal uncertainty was obtained using  $w = 0.6$ . The measured top quark mass is  $M_{top} = 171.5 \pm 1.9(\text{stat}) \pm 2.5(\text{syst}) \text{ GeV}/c^2$ . This represents a 14% improvement in the total uncertainty, compared to the previous CDF result in the same final state. Figure 8 (left) shows the  $M_{hyb}$  distribution for  $b$ -tagged events, with the likelihood fit result superimposed to the observed data.

**5.2. Top quark mass in the lepton plus jets channel.** – D0 recently updated the top quark mass measurement in the lepton plus jets channel using a matrix element technique that calculates the probabilities for each event to come from  $t\bar{t}$  production or background [26]. The overall JES is calibrated *in situ* by imposing a constraint on the mass of the hadronically decaying  $W$  boson. In this measurement D0 uses the full Run II data sample to improve the statistical precision, and also refines the estimation of systematic uncertainties through an updated detector calibration, improvements to the  $b$ -quark JES corrections, and using recent improvements in the modeling of the  $t\bar{t}$  signal. The measured top quark mass is  $M_{top} = 174.98 \pm 0.76(\text{stat} + \text{syst}) \text{ GeV}/c^2$ . This is the most precise Tevatron single measurement of the top quark mass. Figure 8 (right) shows the invariant mass of the jet pair matched to one of the  $W$  bosons. In the ratio of data to SM prediction, the total systematic uncertainty is shown as a shaded band.



## 6. – Conclusions

Tevatron experiments continue providing interesting top quark physics results, even 3.5 years after the end of the Run II data taking. Many top quark areas of study (*i.e.* cross section measurements, single top  $s$ -channel production, spin correlations, production asymmetries) are complementary to LHC measurements. CDF and D0 are in the process of making Tevatron legacy measurements: the current combined top quark mass has an uncertainty already  $< 0.4\%$  and some of the most precise measurements are not yet included in the combination. The final Tevatron single top quark cross section measurements are now available: the observation of the single top quark production in the  $s$ -channel was presented in 2014 and the Tevatron combined  $s + t$  cross section was recently published. The  $t\bar{t}$  production asymmetry measurements have been finalized by both experiments. The tension with the SM observed in the CDF charge asymmetry results is not confirmed by the D0 data.

## REFERENCES

- [1] ABE F. *et al.* (CDF COLLABORATION), *Phys. Rev. Lett.*, **74** (1995) 2626; ABACHI S. *et al.* (D0 COLLABORATION), *Phys. Rev. Lett.*, **74** (1995) 2632.
- [2] ABAZOV V. M. *et al.* (D0 COLLABORATION), *Phys. Rev. Lett.*, **103** (2009) 092001; AALTONEN T. *et al.* (CDF COLLABORATION), *Phys. Rev. Lett.*, **103** (2009) 092002.
- [3] AALTONEN T. *et al.* (CDF and D0 COLLABORATIONS), *Phys. Rev. D*, **89** (2014) 072001.
- [4] CZAKON M. and MITOV A., *Comput. Phys. Commun.*, **185** (2014) 2930.
- [5] ABAZOV V. M. *et al.* (D0 COLLABORATION), *Phys. Rev. D*, **90** (2014) 092006.
- [6] MANGANO M. L., PICCININI F., POLOSA A. D., MORETTI M. and PITTAU ROBERTO, *JHEP*, **07** (2003) 001.
- [7] FRIXIONE S. and WEBBER B. R., *JHEP*, **06** (2002) 029; FRIXIONE S., NASON P. and WEBBER B. R., *JHEP*, **08** (2003) 007.
- [8] KIDONAKIS N., *Phys. Rev. D*, **82** (2010) 114030; KIDONAKIS N., *Phys. Rev. D*, **84** (2011) 011504(R); AHRENS V., FERROGLIA A., NEUBERT M., PECJAK B. D. and LIN YANG L., *JHEP*, **09** (2010) 097.
- [9] CZAKON M., FIEDLER P. and MITOV A., *Phys. Rev. Lett.*, **115** (2015) 052001.
- [10] AALTONEN T. *et al.* (CDF COLLABORATION), *Phys. Rev. D*, **87** (2013) 092002.
- [11] ABAZOV V. M. *et al.* (D0 COLLABORATION), *Phys. Rev. D*, **90** (2014) 072011.
- [12] KUHN J. H. and RODRIGO G., *JHEP*, **01** (2012) 063.
- [13] ABAZOV V. M. *et al.* (D0 COLLABORATION), *Phys. Rev. D*, **92** (2015) 052007.
- [14] AALTONEN T. *et al.* (CDF COLLABORATION), *Phys. Rev. D*, **88** (2013) 072003.
- [15] ABAZOV V. M. *et al.* (D0 COLLABORATION), *Phys. Rev. D*, **90** (2014) 072001.
- [16] TAIT TIM M. P. and YUAN C.-P., *Phys. Rev. D*, **63** (2000) 014018.
- [17] ABAZOV V. M. *et al.* (D0 COLLABORATION), *Phys. Lett. B*, **726** (2013) 656; AALTONEN T. *et al.* (CDF COLLABORATION), *Phys. Rev. Lett.*, **112** (2014) 231804.
- [18] AALTONEN T. *et al.* (CDF and D0 COLLABORATIONS), *Phys. Rev. Lett.*, **112** (2014) 231803.
- [19] KIDONAKIS N., *Phys. Rev. D*, **81** (2010) 054028.
- [20] AALTONEN T. *et al.* (CDF COLLABORATION, D0 COLLABORATION), *Phys. Rev. Lett.*, **115** (2015) 152003.
- [21] KIDONAKIS N., *Phys. Rev. D*, **83** (2011) 091503.
- [22] THE TEVATRON ELECTROWEAK WORKING GROUP for the CDF and D0 COLLABORATION, arXiv:1407.2682.
- [23] THE ATLAS, CDF, CMS, D0 COLLABORATIONS, arXiv:1403.4427.
- [24] AALTONEN T. *et al.* (CDF COLLABORATION), *Phys. Rev. D*, **92** (2015) 032003.
- [25] AALTONEN T. *et al.* (CDF COLLABORATION), *Phys. Rev. D*, **79** (2009) 072005.
- [26] ABAZOV V. M. *et al.* (D0 COLLABORATION), *Phys. Rev. Lett.*, **113** (2014) 032002.